Microbial Cell Factories

RESEARCH Open Access

# Enhanced protein secretion in reduced genome strains of *Streptomyces lividans*

Mohamed Belal Hamed[1,2,7], Tobias Busche[3], Kenneth Simoens[4], Sebastien Carpentier[5], Jan Kormanec[6], Lieve Van Mellaert[1], Jozef Anné[1], Joern Kalinowski[3], Kristel Bernaerts[4], Spyridoula Karamanou[1*] and Anastassios Economou[1†]

## Abstract

**Background** *S. lividans* TK24 is a popular host for the production of small molecules and the secretion of heterologous protein. Within its large genome, twenty-nine non-essential clusters direct the biosynthesis of secondary metabolites. We had previously constructed ten chassis strains, carrying deletions in various combinations of specialized metabolites biosynthetic clusters, such as those of the blue actinorhodin (*act*), the calcium-dependent antibiotic (*cda*), the undecylprodigiosin (*red*), the coelimycin A (*cpk*) and the melanin (*mel)* clusters, as well as the genes *hrdD*, encoding a non-essential sigma factor, and *matAB*, a locus affecting mycelial aggregation. Genome reduction was aimed at reducing carbon flow toward specialized metabolite biosynthesis to optimize the production of secreted heterologous protein.

**Results** Two of these *S. lividans* TK24 derived chassis strains showed ~ 15% reduction in biomass yield, 2-fold increase of their total native secretome mass yield and enhanced abundance of several secreted proteins compared to the parental strain. RNAseq and proteomic analysis of the secretome suggested that genome reduction led to cell wall and oxidative stresses and was accompanied by the up-regulation of secretory chaperones and of *secDF*, a Sec-pathway component. Interestingly, the amount of the secreted heterologous proteins mRFP and mTNFα, by one of these strains, was 12 and 70% higher, respectively, than that secreted by the parental strain.

**Conclusion** The current study described a strategy to construct chassis strains with enhanced secretory abilities and proposed a model linking the deletion of specialized metabolite biosynthetic clusters to improved production of secreted heterologous proteins.

**Keywords** Reduced genome strains, Secretome, Proteomics, Transcriptomics, Heterologous secretion

†Deceased, 3 July 2023.

*Correspondence:
Spyridoula Karamanou
lily.karamanou@kuleuven.be
[1]Department of Microbiology, Immunology and Transplantation, Rega Institute, Laboratory of Molecular Bacteriology, KU Leuven, Herestraat 49, Leuven B-3000, Belgium
[2]Molecular Biology Depart, National Research Centre, Dokii, Cairo, Egypt
[3]Center for Biotechnology (CeBiTec), Bielefeld University, Bielefeld, Germany
[4]Department of Chemical Engineering, Chemical and Biochemical Reactor Engineering and Safety (CREaS), KU Leuven, Leuven B-3001, Belgium
[5]SYBIOMA, KU Leuven facility for Systems Biology Based Mass Spectrometry, Leuven B-3000, Belgium
[6]Institute of Molecular Biology, Slovak Academy of Sciences, Dubravska cesta 21, Bratislava 84551, Slovakia
[7]Department of Neurosciences, Leuven Research Institute for Neuroscience and Disease (LIND), KU Leuven, VIB-KU Leuven Center for Brain & Disease Research, Leuven, Belgium

## Background

*Streptomyces* is a ubiquitous soil microorganism, known for its ability to secrete polypeptides and specialized metabolites [1, 2]. The lack of an outer membrane and the low level of secreted proteases makes it an attractive platform for heterologous polypeptide production [3] like tumor necrosis factor-alpha [4, 5], xyloglucanase [6], cellulase A [2], phospholipase D [7], glutenase [8] and red fluorescent protein [3].

The solved chemical structures of specialized metabolites (<30% solved; [9]) are highly diverse and include polyketides, peptides, pyrones, oligopyrroles, γ-butyrolactones, butenolides, furans, terpenoids, fatty acids, nucleosides and deoxysugars. Various pathways are involved in the biosynthesis of these specialized metabolites including polyketide [10] as well as ribosomal and non-ribosomal peptide synthases [11, 12], shikimate [13], β-lactam [14] and carbohydrate [12] whose expression varies with environmental conditions [15]. The genes involved in specialized metabolite biosynthesis are usually clustered. The number of clusters varies between species; 37 and 29 clusters were detected *in silico* in *S. avermitilis* [16] and *S. lividans* TK24/ *S. coelicolor* A3 (2) genomes, respectively [16–18]. The clusters directing the biosynthesis of polyketides (*act*, *cpk*A), peptidic (calcium-dependent ionophore, *cda*) and hybrid peptidic/polyketide (*red*) antibiotics are the best characterized. These antibiotics are highly produced by *S. coelicolor* and poorly produced by *S. lividans* [19]. Cluster-situated transcriptional activators, regulate expression of the various pathways [20, 21]. The most frequently encountered ones are the *Streptomyces* antibiotic regulatory proteins (SARPs) [22]. For the *act*, *red*, *cda* and *cpk* clusters the respective SARPs are ActII-ORF4, RedD, CdaR, and CpKO [16]. The transcription of ActII-ORF4 and RedD in *S. coelicolor* A3(2) is initiated by an RNA polymerase holoenzyme containing the non-essential sigma factor *hrdD* [23–25]. The upregulation of the SARPs expression coincides with morphological and physiological differentiation [26]. In *S. coelicolor*, the transcription of *redD* and *cdaR* doubles during the exponential phase, while that of *act*II-*ORF4* gene increases before entering the stationary phase [27].

Several reduced genome strains were generated to improve bacterial metabolic efficiency [28, 29] and these manipulations led unexpectedly to growth rate reduction as well as enhanced protein secretion [30]. For instance, the deletion of non-essential *E. coli* genes, in a step-wise manner (from 48 to 982 kb), revealed a positive correlation between genome shortening and slow growth [31]. In *Bacillus subtilis*, the deletion of 11 non-essential clusters (865 genes) was correlated with the enhanced secretion of heterologous cellulase and M-protease [32] and a 20.7% reduction of the genome of this strain led to two-fold increase in the secretion of alkaline cellulase Egl237 [33]. A reduction of only 2.8% of the *Lactococcus lactis* NZ9000 genome (including prophages, transposons, and related proteins) led to a two-fold increase in the secretion of red fluorescent protein [34].

Many attempts were made to construct reduced genome *Streptomyces* strains with the aim to improve precursors supply for the optimal biosynthesis of target heterologous proteins and antibiotics [35–37]. In doing so, specific proteases and specialized metabolite genes were deleted [24, 36–38]. A *Streptomyces* strain missing the zinc metalloprotease FtsH secreted 29 folds more mRFP than the original strain [37]. A *S. coelicolor* derivative strain missing 10 polyketide and non-ribosomal peptide clusters showed 6 folds enhanced production of actinorhodin compared to the original strain [39]. Another *S. coelicolor* derived strain deleted for the *act*, *red*, *cpk* and *cda* clusters showed an enhanced heterologous production of chloramphenicol and congocidin [40] or of the antitumoral polyketide mithramycin A [38].

We have previously deleted 5 specialized metabolite clusters and 3 individual genes from *S. lividans* TK24, in various combinations, generating 10 reduced genome strains (hereafter RG; Fig. 1; Table 1 and S1) [35, 38]. The deleted clusters were those directing the biosynthesis of the specialized metabolites *cda, cpk*, *red* and *act* as well as the gene encoding for the sigma factor *hrdD* involved in their transcription (Fig. 1). Furthermore, since melanin

**Table 1** Reduced genome strains with the indicated gene/cluster deletions. Details in Table S1

| No. | Strain name | Deleted clusters and genes | | | | | | |
|---|---|---|---|---|---|---|---|---|
| 1 | TK24(RG1.0) | | | *act* | | | | |
| 2 | TK24(RG1.1) | | *red* | *act* | | | | |
| 3 | TK24(RG1.3) | | *red* | *act* | *cda* | | | |
| 4 | TK24(RG1.4) | *cpk* | *red* | *act* | *cda* | | | |
| 5 | TK24(RG1.5) | | *red* | *act* | | | *hrdD* | |
| 6 | TK24(RG1.6) | | *red* | *act* | *cda* | *mel* | | |
| 7 | TK24(RG1.7) | *cpk* | *red* | *act* | *cda* | *mel* | | |
| 8 | TK24(RG1.8) | | *red* | *act* | *cda* | *mel* | *hrdD* | |
| 9 | TK24(RG1.9) | | *red* | *act* | *cda* | *mel* | | *matAB* |
| 10 | TK24(RG1.10) | *cpk* | *red* | *act* | *cda* | *mel* | | *matAB* |

and extracellular glycan can impact negatively the production and industrial bioprocessing of heterologous secreted proteins [38, 41], the genes responsible for their biosynthesis (*mel* and *mat*A/B respectively) were also deleted.

We show here that the secretome of these reduced genome strains differ from that of the parental strain. These strains exhibit an improved capacity to produce and secrete both native and heterologous proteins compared to the parental strain. Our study led to a better understanding of the connection between the deletion of specialized metabolite clusters and the enhanced production of secreted proteins.

## Materials and methods

### Strains, media and vectors used in the study

*Streptomyces lividans* TK24 was used as a wild-type strain [2, 42]. Protoplast formation and subsequent transformation were as described [43, 44]. Deletion of specialized metabolite clusters to generate reduced genome strains (RG) was carried out as described [35, 38].

Phage medium, Minimal Medium (MM), Minimal Medium with 5 g Bacto casamino acids/L ($MM_{C5}$) and Nutrient Broth (NB) without NaCl, were as described [2, 3, 45]. Solid medium MRYE was as previously described [44]. Whenever necessary, media were supplemented with thiostrepton (for liquid 10 µg/µL ; for solid 50 µg/µL) [2] .

### Growth conditions

*S. lividans* TK24 and derivatives were incubated in Phage medium (50 ml) supplemented with thiostrepton (10 µg/ml), at 28 °C, for 48 h, with continuous shaking (240 rpm). The optical density ($OD_{600}$) of precultures was measured. Mycelia were harvested (3800 x g; 15 min; SIGMA 3-16 K centrifuge), washed twice with sterile water and homogenized in 50 mL sterile water. Strains were then inoculated into 250-mL Erlenmeyer flasks containing 100 mL of nutrient broth medium (NB). To secure the same amount of mycelia per inoculum was used we followed this formula: [volume of inoculum= (Final volume of culture X 0.25)/ $OD_{600}$] [3]. The flasks were shaken at 240 rpm, at 28 °C; the pH was controlled using 100 mM MES buffer (pH 6.9).

mRFP and mTNFα production in all strains was achieved as described in [2, 3, 6].

### Dry cell mass determination

For dry cell weight (DCW) determination, 10 mL of cultures were centrifuged (3800 x g; 15 min; SIGMA 3-16KL). Bacterial pellets were resuspended in sterile water and filtered under vacuum using pre-dried and pre-weighted 0.2 µm filters (PORAFIL® MV; Macherey-Nagel). Filters were then re-dried (12–24 h; at 60°C) and re-weighted.

### Fluorescence assays and quantification of fluorescent proteins

To evaluate strain performance, we compared the mRFP fluorescence intensity of the different cultures at their transition point to stationary phase (excitation: 550 nm; emission: 580 nm; Infinite® M200 microplate reader; Tecan). Error propagation was applied to calculate DCW-specific mRFP production.

Quantification of mRFP using purified His-mRFP was as described [3]. The amounts of mRFP detected via fluorescence assays were then compared to those quantified by western blots using antibodies against mRFP (see western blot analysis below).

### SDS-PAGE and Western blot analysis

Following centrifugation of cultures (10 min, 4200 x g, 4 °C), proteins in the spent medium were precipitated by trichloroacetic acid (TCA; final concentration of 20% w/v; 4 °C). Extracellular proteins were separated by SDS-PAGE using the Precision Plus Protein™ Standard (All Blue) marker from Bio-Rad [46, 47] and visualized by silver staining or immuno-detection. mRFP and mTNFα polyclonal antibodies were raised in rabbits against lab-purified proteins at Davids Biotechnologie, Germany. Immunodetection was carried out using the GE Healthcare Amersham ECL reagents and ImageQuant LAS 4000 Imager. High-resolution images were processed using ImageJ as described in [2].

### Secretomics sample preparation and measurement

Cell removal and protein precipitation were as previously described [3, 45]. The protein pellet was solubilized in 8 M Urea −1 M ammonium bicarbonate solution (ABS). Protein concentration was measured using the Bradford reagent. Polypeptides (3 µg) were separated by 12% SDS-PAGE and visualized by silver staining (Shevchenko et al. 1996).

### Analysis of secretomes by nanoLC-MS/MS

A volume corresponding to the secreted polypeptides derived from $3\times10^6$ cells (usually a volume equivalent to 20–40 µL of the initial cell culture) was used for in-solution tryptic digestion. The protein solution was initially diluted into urea (2 M final concentration in 50 mM Ammonium bicarbonate solution (ABS), followed by reduction of cysteines with 1 mM DTT (45 min; 56 °C), alkylation using 10 mM Iodoacetamide (IAA) (45 min; 22 °C; dark) and digestion using 0.015 µg Trypsin for 1.5 µg protein (Trypsin Gold, Promega, Fitchburg, Wisconsin; ratio trypsin/protein 1/100; overnight; 37 °C). Digested peptide solutions were acidified with trifluoroacetic acid

(TFA) to pH < 2, desalted using STAGE tips [48, 49], and stored lyophilized at -20 °C, until the MS analysis.

Lyophilized peptide samples were re-suspended in an aqueous solution containing 0.1% v/v formic acid (FA) and 5% v/v Acetonitrile (ACN) and analyzed using nano-Reverse Phase LC coupled to a QExactive Hybrid Quadrupole - Orbitrap mass spectrometer (Thermo Scientific, Bremen, Germany) through a nanoelectrospray ion source (Thermo Scientific, Bremen, Germany). Peptides were initially separated using a Dionex UltiMate 3000 UHPLC system on an EasySpray C18 column (Thermo Scientific, OD 360 µm, ID 50 µm, 15 cm length, C18 resin, 2 µm bead size) at a flow rate of 300 nL $min^{-1}$. The LC mobile phase consisted of two different buffer solutions, an aqueous solution containing 0.1% v/v FA (Buffer A) and an aqueous solution containing 0.08% v/v FA and 80% v/v ACN (Buffer B). A 60 min multi-step gradient was used from Buffer A to Buffer B as follows [0–3 min constant (96:4), 3–15 min (90:10); 15–35 min (65:35); 35–40 min (35:65); 40–41 min (5:95); 41–50 min (5:95); 50–51 min (95:5); 51–60 min (95:5)].

The separated peptides were analyzed in the Orbitrap QE operated in positive ion mode (nanospray voltage 1.5 kV, source temperature 250 °C). The instrument was operated in data-dependent acquisition (DDA) mode with a survey MS scan at a resolution of 70,000 FWHM for the mass range of m/z 400–1600 for precursor ions, followed by MS/MS scans of the top 10 most intense peaks with +2, +3 and +4 charged ions above a threshold ion count of 16,000 at 35,000 resolution. MS/MS was performed using normalized collision energy of 25% with an isolation window of 3.0 m/z, an apex trigger 5–15 s and a dynamic exclusion of 10 s. Data were acquired with Xcalibur 2.2 software (Thermo Scientific).

Raw MS files were analyzed by the MaxQuant v1.5.3.3 proteomics software package (Cox, Mann 2008). MS/MS spectra were searched by the Andromeda search engine against the Uniprot *S. lividans* TK24 proteome (taxonomy: 457,428, last modified 2020, 7520 protein entries; [17] and common contaminants (e.g. trypsin, keratins). Enzyme specificity was set to trypsin and a maximum of two missed cleavages were allowed. Dynamic (methionine oxidation and N-terminal acetylation) and fixed (S-carbamidomethylation of cysteinyl residues) modifications were selected. Precursor and MS/MS mass tolerance was set to 20 ppm for the first search (for the identification of the maximum number of peptides for mass and retention time calibration) and 4.5 ppm for the main search (for the refinement of the identifications). Protein and peptide false discovery rate (FDR) were set to 1%. FDR was calculated based on the number of spectra matched to peptides of a random proteome database (reversed sequence database) in relation to the number of spectra matching to the reference proteome. Peptide features were aligned between different runs and masses were matched ("match between runs" feature), with a match time window of 3 min and a mass alignment window of 20 min. Protein quantification was performed using the iBAQ algorithm [50] through MaxQuant software. Differentially abundant proteins were selected using the t-test and by comparing the fold difference of average protein intensities between the samples. P-values were further corrected for multiple hypothesis testing error using the Benjamini-Hochberg method [51].Thresholds for the analysis were set to adjusted p-value < 0.05 and fold difference > 2. Functional characterization of proteomics results was performed after filtering the dataset only to secreted proteins, excluding cytoplasmic contamination, using proteome annotation as described in the SToPSdb [52] (www.stopsdb.eu). The percentage of differentially abundant proteins that match a specific term over the total differentially abundant proteins for each condition was plotted. Keywords were derived after manual curation of the proteome.

#### RNA isolation and differentially expressed genes

Samples for transcriptomics data analysis were taken during the late-exponential growth phase. The cells were grown in NB medium and the harvesting and RNA isolation was performed using Trizol reagent (Invitrogen) following the manufacturer's instructions, and was treated with DNase I (Invitrogen) to remove chromosomal DNA contamination [53]. Samples of 5 different biological replicates for each strain were isolated separately and pooled after quality control. The RNA quality was checked, and the TruSeq Stranded mRNA Library Prep Kit was done as described in [45, 54, 55].

Transcriptomics analysis and differential expression were carried out as described in [56]. In brief raw FASTQ files were processed using the CLC Genomics Workbench (CLC Bio, Aarhus, Denmark). Raw reads were trimmed by their overall quality (score: 0.05; maximum ambiguous nucleotides: (2) and length (minimum length: 15 nucleotides). The filtered reads were mapped to *S. lividans* TK24 genome sequence, accession number (NZ_CP009124), with the default parameters (mismatch cost: 2; insertion cost: 2; deletion cost: 3; length fraction: 0.9; similarity fraction: 0.9; and ignore non-specific matches). The read counts were normalized using the DESeq-2 package in R [57].

Reads per kilobase per million mapped reads (RPKM) [58] were calculated based on the raw read counts per CDS. Differential gene expression analysis was performed using ReadXplorer v2.2 [59] using DESeq2 [57]. The signal intensity value (A-value) was calculated by the average ($log_2$) RPKM of each gene and the signal intensity ratio (M-value) by the difference of ($log_2$) TPM. The differential RNA-Seq data was evaluated using an adjusted

P-value cut-off of $P \leq 0.05$ and a signal intensity ratio (M-value) cut-off of $\geq +1$ or $\leq -1$ (fold-change of $\pm 2$).

### Metabolomics analysis

Exometabolomics analysis was performed on triplicate cultures of *S. lividans* TK24 wildtype and RS1.9 grown in nutrient broth. At several time points, free amino acid concentrations in the medium were measured. Cells were removed by centrifugation (4500 x g for 5 min) followed by microfiltration (syringe filter, 0.2 µm, cellulose acetate). Free amino acids were determined with the EZ:FAAST amino acid analysis kit of Phenomenex on a GC-FID (Perkin Elmer) according to supplier instructions. Measured amino acids are: alanine (ALA), glycine (GLY), α-amino-butyrate (ABA), valine (VAL), β-amino-isobutyric acid (BAIB), leucine (LEU), isoleucine (ILE), threonine (THRE), serine (SER), proline (PRO), asparagine (ASN), aspartate (ASP), methionine (MET), hydroxyproline (HYP), glutamate (GLU), phenylalanine (PHE), α-amino-adipic acid (AAA), glutamine (GLN), ornithine (ORN), cysteine (CYS), lysine (LYS), histidine (HIS), tyrosine (TYR), tryptophan (TRP). BAIB, HYP, AAA, GLN, ORN, and CYS were left out of the PCA analysis as these data were either too noisy or the amino acids were not really used as substrates. Principal component analysis was performed in MATLAB R2016b (The Mathworks) using included functions.

### Miscellaneous

Chemicals (Sigma), Bacto Soytone (DIFCO Laboratories), DNA enzymes (New England Biolabs) and oligonucleotides (Eurogentec) were used.

The mass spectrometry proteomics data have been deposited to the ProteomeXchange Consortium via the PRIDE partner repository [60] with the dataset identifiers PXD040146.

Submission details:

*Project Name: Enhanced protein secretion in reduced genome strains of Streptomyces lividans.*
*Project accession: PXD040146.*
*Reviewer account details:*
*Username: reviewer_pxd040146@ebi.ac.uk.*
*Password: 1uBKUTp6.*

## Results

### Transcription of specialized metabolite clusters/genes in *S. lividans* TK24

The transcription levels of the clusters/ genes that had been deleted in the RG strains (Fig. 1) were monitored in the *S. lividans* TK24 parental strain during growth in minimal medium supplemented with glucose [2, 3, 24, 37]. Samples were collected at three distinct growth phases (early-/ late-exponential and stationary) and transcriptomes analysed using RNAseq. Results are presented in Fig. S1 and Table S2. Under these conditions, the transcript level for most of the specialized metabolite biosynthetic genes was high at the late-logarithmic phase (Fig. S1). The *act* cluster (*SLIV_12925* to *SLIV_13030*) showed the highest transcript levels in both late-exponential and stationary phases. Specialized metabolite regulatory proteins (SARPs), antibiotics cluster activators [61], *red*Z (*SLIV_09200*), *red*D (*SLIV_09220*) and *cda*R (*SLIV_21605*) showed high transcript levels in the late-log phase (in red). The *act*II-*ORF4* (*SLIV_12960*) showed the highest transcript levels in both late-exponential and stationary phases (in red). On the other hand, *cpk*O (*SLIV_06745*) and *cpk*N (*SLIV_06705*), showed moderate transcript levels during all growth phases (in red). The upregulation of SARPs is consistent with previous reports in *S. coelicolor* A3(2) [62], despite differences in the level of expression among the two strains [63].


**Fig. 1** Physical maps of the chromosomal regions deleted in *S. lividans* TK24
The regions corresponding to the actinorhodin (26.7 kb), undecylprodigiosine (39.3 kb), calcium dependent antibiotic (26.7 kb), coelimycin P1 (59.1 kb) and melanin (8.9 kb) biosynthetic clusters as well as those encoding for the transcription factor HrdD (1.3 kb) and aggregation genes *mat*AB (4.5 kb) were deleted in various combinations

### Effect of cluster/gene deletions on cell growth and native secretome

The effect of cluster/gene deletions on cell growth was tested for all the engineered strains. We used nutrient broth (NB) as it has been previously described as the best-performing medium for native and heterologous protein production [2, 3, 37]. For each strain, the same amount of mycelia was used as inoculum (see formula in Materials and methods). Most strains showed a growth pattern similar to that of the parental strain (Fig. S2A). However, 7 among them yielded slightly lower and 2 yielded slightly higher amount of dry cell weight (DCW; g/L), at late exponential phase, than the parental strain (Fig. 2A). The slower growth rate of some RG strains might be attributed to the rapid consumption/ eventual depletion from the medium, of aspartate, glutamate and asparagine, as seen for RG1.9 (Fig. S5; Table S7).

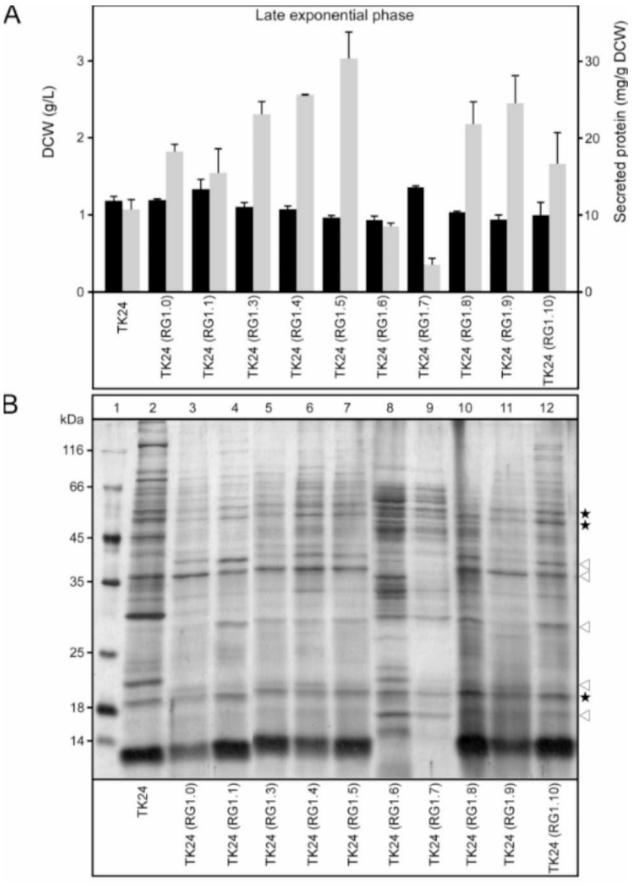


**Fig. 2** Total biomass and native secretome yield in *S. lividans* TK24 and reduced genome derivative strains. **(A)** Dry cell weight (DCW; g/L; black bars) and total secretome yield (mg secreted protein/ g DCW; grey bars) following growth of the indicated strains in nutrient broth (NB) until late exponential phase. $n=3$; values represent the mean ± SD; **(B)** Equal amount of secreted polypeptides (3 µg/lane) from the indicated strains, grown as in A, were analyzed by SDS-PAGE and silver stained. Lane 1: molecular weight marker. Proteins with major (arrows)/ little (asterisks) change among strains are indicated

To determine the effect of cluster/gene deletions on the native secretome, the amount of total native secretome produced by each strain per gram of dry cell weight (DCW) was estimated. The secretome mass produced by 8 of the 10 strains was higher than that produced by the parental strain (Fig. 2A). The highest mass was obtained from RG1.5 and was 3 folds higher than that of the parental strain (~30 mg/g DCW). RG strains 1.3, 1.4, 1.8 and 1.9 produced 2 folds more, whereas RG strains 1.6 and 1.7 produced less, secretome mass than the parental strain (Fig. 2A). Our results confirm previously reported correlation between slow growth rate and enhanced protein secretion [2, 3, 45].

To study the impact of deletions on the native secretome profile, following growth in NB medium for 24 h, the secreted polypeptides of all 11 strains were TCA precipitated, analyzed by SDS-PAGE and silver stained (Fig. 2B). While the abundance of some proteins was similar between strains (asterisks), that of others changed in some RG strains (arrows). Some new polypeptides appeared in RG strains while others were lost.

To accurately determine the nature of the changes, the secretomes of the parental strain (TK24) and of three RG strains (1.4, 1.5, 1.9; that produced the highest native secretome mass; Fig. 2A) were compared by label-free nanoLC-MS/MS. Polypeptides were identified and quantified (Fig. 3 and S3; Tables S3 and S4). The abundance of each protein (units/ mg DCW) in the RG strains was compared to that of the parental strain (Fig. 3 and S3). Several secreted polypeptides (~10–15% of a secretome) were statistically differentially abundant (lower or higher); i.e. 62 proteins in RG1.4, 55 in RG1.5 and 86 in RG1.9. Out of them, 39 proteins in RG1.4, 36 in RG1.5 and 67 in RG1.9 were more abundantly secreted in the RG strains than in the parental strain (Fig. 3 and S3; Table S4). Examples of proteins whose secretion levels were affected include a putative lipoprotein of the LolA/LolB/LppX family and a N-acetylmuramoyl-L-alanine amidase that were secreted 1.6 and 3 folds more, respectively, by all of the RG strains than by the parental one. Phospholipase A2 (D6ES51) and A0A076MBH5 of unknown function secreted through the Tat pathway, were secreted respectively 1.5 and 6 folds less by the RG strains than by the parental strain.

The secreted proteins that showed differential abundance between mutants and parental strain fell into six main functional classes (Fig. 3C and D and S4). Proteins with hydrolytic functions were oversecreted in all RG strains examined [e.g. Amidase (*SLIV_06435*), putative phosphodiesterase (IPR017946) (*SLIV_27875*) and probable subtilinase-type protease inhibitor (*SLIV_34120*)] (RG1.4, 1.5, 1.9; Fig. 3C and D and S4). Hydrolases, peptidases and proteases were mainly over-secreted in RG1.9. These include two metallopeptidases (*SLIV_01290*

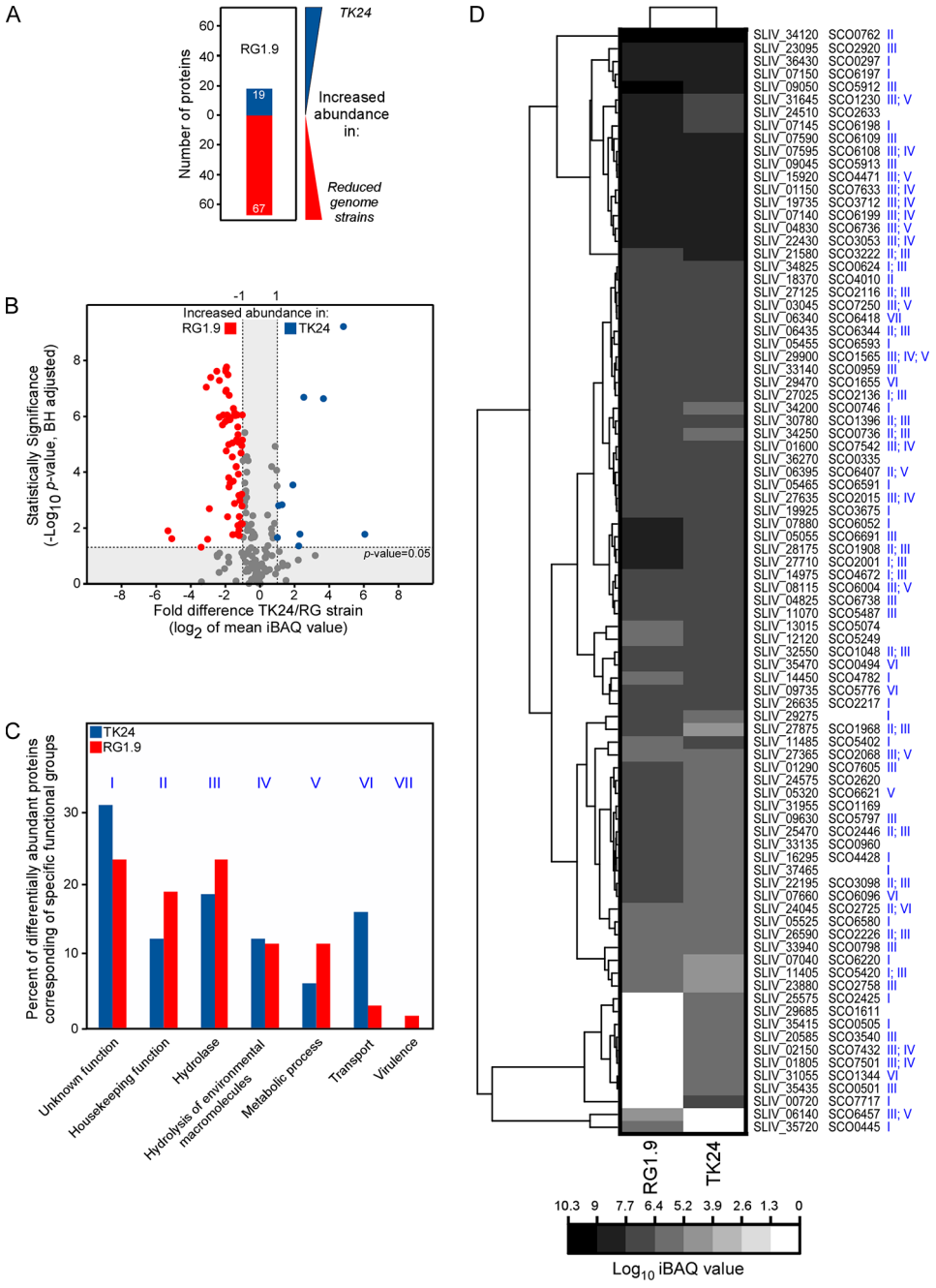


**Fig. 3** Comparative secretome analysis of *S. lividans* TK24 and RG1.9 strains. **(A)** Proteins secreted by the parental and by the RG1.9 strains were differentially abundant. Blue: more abundant in the parental strain; red: more abundant in the RG1.9 strain. The secretome amount that was produced by a fixed amount of cell biomass was loaded for both strains for proteomics analysis. **(B)** The summary of proteins that were differentially abundant in the secretome of the parental and the RG1.9 strains is shown as volcano plots (for detailed description see panel C and Table S1). Each dot represents one protein. Blue: more abundant in the parental strain; Red: more abundant in the RG1.9 strain. Plotted on the *x* axis is the fold difference (in $\log_2$ scale) of the mean protein abundance in the parental strain over that in RG1.9, and on the *y* axis the *p*-value derived from a *t*-test between the two strains ($-\log_{10}$, adjusted from [64]. **(C)** Classification of the differentially abundant proteins based on their biological function, as described [52]. The ratio 'number of differentially abundant proteins that belong to the indicated functional group/ total number of differentially abundant proteins in the same strain' is plotted. The dataset was filtered in order to retain secreted proteins and eliminate contaminating cytoplasmic proteins. Functional groups are coded with latin numbers as indicated. **(D)** Clustering of iBAQ values for proteins that showed differential abundance in the secretome of the parental and of the RG1.9 strains. Proteins have been annotated with both *S. lividans* TK24 (SLIV) and *S. coelicolor* (SCO) gene IDs. Latin numbers next to gene IDs indicate protein functions as these were grouped in panel C

and *SLIV_04830*), two proteases (SLIV_09050 and *SLIV_09045*), a peptidase (*SLIV_04650*) containing LysM (IPR018392) and M23 (IPR016047) domains, two glycoside hydrolases (*SLIV_33135* and *SLIV_34355*) (Fig. 3C and S4; Table S4). All subsequent experiments were done with the RG1.9 strain that exhibited the highest number of differentially abundant proteins compared to the parental strain.

Our proteomics analysis revealed that the RG1.9 strain over-secreted 40 proteins with hydrolytic function including 13 proteins that are likely to target the cell wall. More specifically these include: a D-Ala-D-Ala dipeptidase (D6EQU5), a protein with lysozyme-like (IPR023346) (D6EKB6) and LysM (IPR018392) domains (D6ETM1) and a gamma-glutamyltransferase (D6EID2) that were secreted *via* the Sec pathway, and the beta-N-acetylhexosaminidase (A0A076M9V2) and L, D-transpeptidase (D6EYE3) that were secreted *via* the Tat pathway (Tables S3 and S4). The RG1.9 strain also over-secreted a protein with redox-related function. Collectively, our observations suggest that the *S. lividans* derived strains bearing deletions of the genes mentioned above have an enhanced ability to secrete hydrolytic proteins involved in the remodeling of the cell wall.

### Effect of cluster/gene deletions on transcription

The differences between the native secretome profiles of the parental *S. lividans* TK24 and the RG strains could be explained by enhanced transcription of genes encoding the secreted proteins and/or of genes encoding chaperones or components of the secretion apparatus.

In order to clarify these points, we compared the transcriptomes of the parental and RG1.9 strains, both grown in NB. 349 genes out of a total of 7306 genes showed differential expression between the two strains (signal intensity ratio M-value > 1; adjusted *p*-value < 0.05; see materials and methods; Fig. 4; Table S6). Out of these, 196 were upregulated in RG1.9, encoding 132

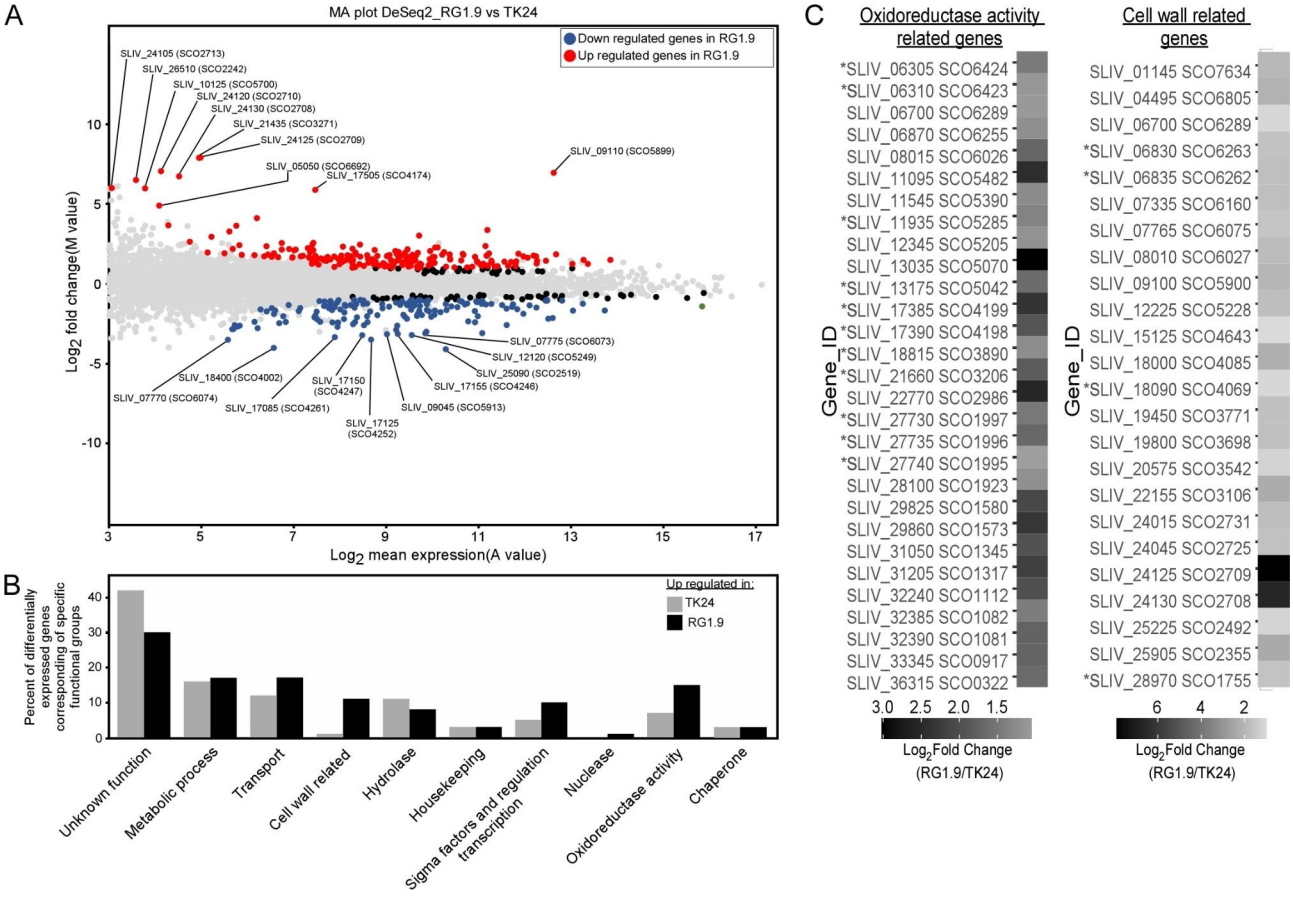


**Fig. 4** Differential expression of genes between *S. lividans* TK24 and RG1.9 strains. **(A)** MA-plot for RNA-Seq datasets comparing *S. lividans* TK24 and RG1.9 strains. Genes similarly regulated in both strains (grey) and up- (red) or down- (blue) regulated in RG1.9 are indicated (M > 1 or M <-1 respectively; adjusted *p*-value < 0.05). M and A values were calculated as indicated (Material and Methods). For the 10 most prominently up- / down- regulated genes their SLIV/SCO gene IDs are indicated. **(B)** Differential expression of genes encoding proteins with the indicated biological function (as described, [52]) in *S. lividans* TK24 (grey) and RG1.9 (black) strains. For each strain and each functional group, the ratio 'number of differentially expressed genes / total number of genes' was plotted. **(C)** Heatmap of genes related to oxidoreductase (left) or cell wall (right) functions that were upregulated in RG1.9, classified as in panel B. Annotations with SLIV/ SCO gene IDs are indicated. Asterisks: genes that belong to the $Sig^R$ or $Sig^E$ regulons

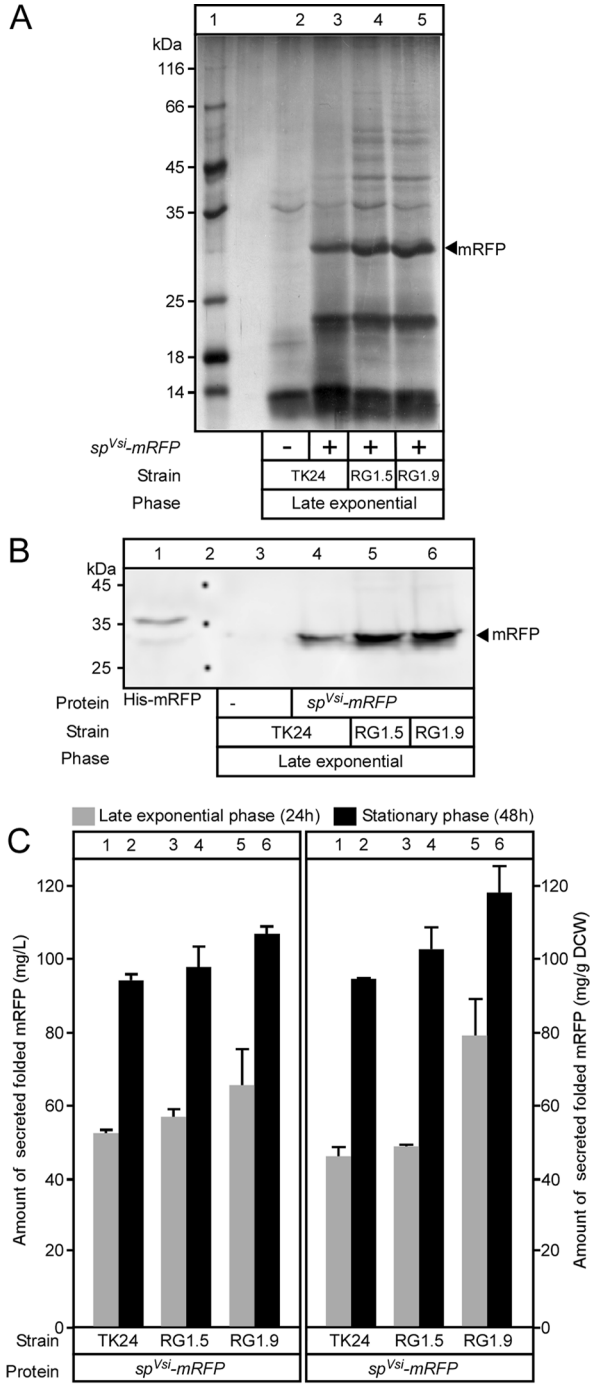


**Fig. 5** Effect of cluster/gene deletions on heterologous protein secretion. **(A)** Strains carrying pIJ486/*sp*$^{Secv}$*-mRFP*, as indicated, were grown in NB for 24 h. Secreted proteins were TCA precipitated, analyzed by SDS-PAGE and silver stained. Lanes were loaded with 5–10 µL of collected polypeptides, a volume corresponding to 0.1 mg DCW. Lane 1: Molecular weight marker; Arrow; mRFP, as indicated. **(B)** Immunostaining of the samples presented in Panel A (same sample loading) using mRFP specific antibodies. Lane 1: purified his-mRFP; Lane 2: molecular weight marker. **(C)** The amounts of mRFP secreted by the *S. lividans* TK24 and RG strains (as indicated), grown in NB medium, for 24 (grey) or 48 h (black bars), were expressed either in mg/L (left panel) or in mg/gram of DCW (right panel). $n = 3$, values represent the mean ± SD

cytoplasmic, 40 membrane, 5 nucleoid/ ribosomal and 14 secreted proteins. All genes that showed differential expression between the parental and the RG strain were classified into 10 functional groups; 6 of them were upregulated in RG1.9 (Fig. 4B, Table S6).

Interestingly, a gene encoding for the bifunctional translocase subunit SecDF, an important component of the Sec export system, was upregulated 1.8-folds in RG1.9 (Table S6) whereas none of the Tat-pathway component genes were affected. Furthermore, four genes encoding proteins involved in stress response.

were significantly upregulated (up to 1.5 fold) in RG1.9 (Table S6). These include the putative proteasome assembly chaperone 2 (IPR019151), the ATP-dependent serine protease Lon (D6EUK1) [65], the thioredoxin reductase A (D6EMA7) [66] and the nitrate reductase subunit delta (D6EHT8) belonging to the OsdR regulon [67] (Table S6).

Interestingly, among the genes upregulated in the RG strain 20 were related to cell wall function [e.g. the genes encoded for Peptidoglycan biosynthesis protein MurJ (IPR004268) (*SLIV_24125*) and O-antigen ligase-related (IPR007016) (*SLIV_24130*)] (Fig. 4B-C; Table S6; marked with one asterisk). Four of them are known to be under the control of the sigma factor Sig$^{E}$, involved in the cell envelope stress response [68]. Eighteen additional genes encoded proteins annotated as oxidoreductase activity (Fig. 4B-C; Table S6; marked with two asterisks); 11 of them belonged to the Sig$^{R}$ regulon involved in redox homeostasis [69]. Finally, four genes of the arginine biosynthesis pathway (Table S6; marked with three asterisks) that forms arginine from glutamate [70], showed upregulation [1.3–2.3 folds; *argH* (*SLIV_29875*), *argC* (*SLIV_29825*), *argJ* (*SLIV_29830*) and *argG* (*SLIV_04065*)]. These genes may play a key role in cell-wall biosynthesis, since glutamine derived from glutamate is a major component of peptidoglycan. Alternatively, one cannot exclude that arg biosynthesis is required for the enhanced efficiency of the Twin-arginine translocation pathway in *S. lividans* [71–75]. These data indicated that deletion of *red*, *act*, *cda* and *mel* clusters and of the *matAB* genes in the RG1.9 strain led to cell wall and oxidative stresses.

### Effect of cluster/gene deletions on heterologous protein secretion

Finally, we tested whether genome reduction impacted secretion of heterologous polypeptides. The monomeric red fluorescence protein, tagged with a histidine tag and fused to the *vsi*-encoded signal sequence, was cloned behind the *vsi* promoter in the high copy number plasmid pIJ486 to produce pIJ486/*sp*$^{SecV}$*-mRFP* [3]. This plasmid was transformed via protoplast transformation (see materials and methods) in *S. lividans* TK24 and two RG

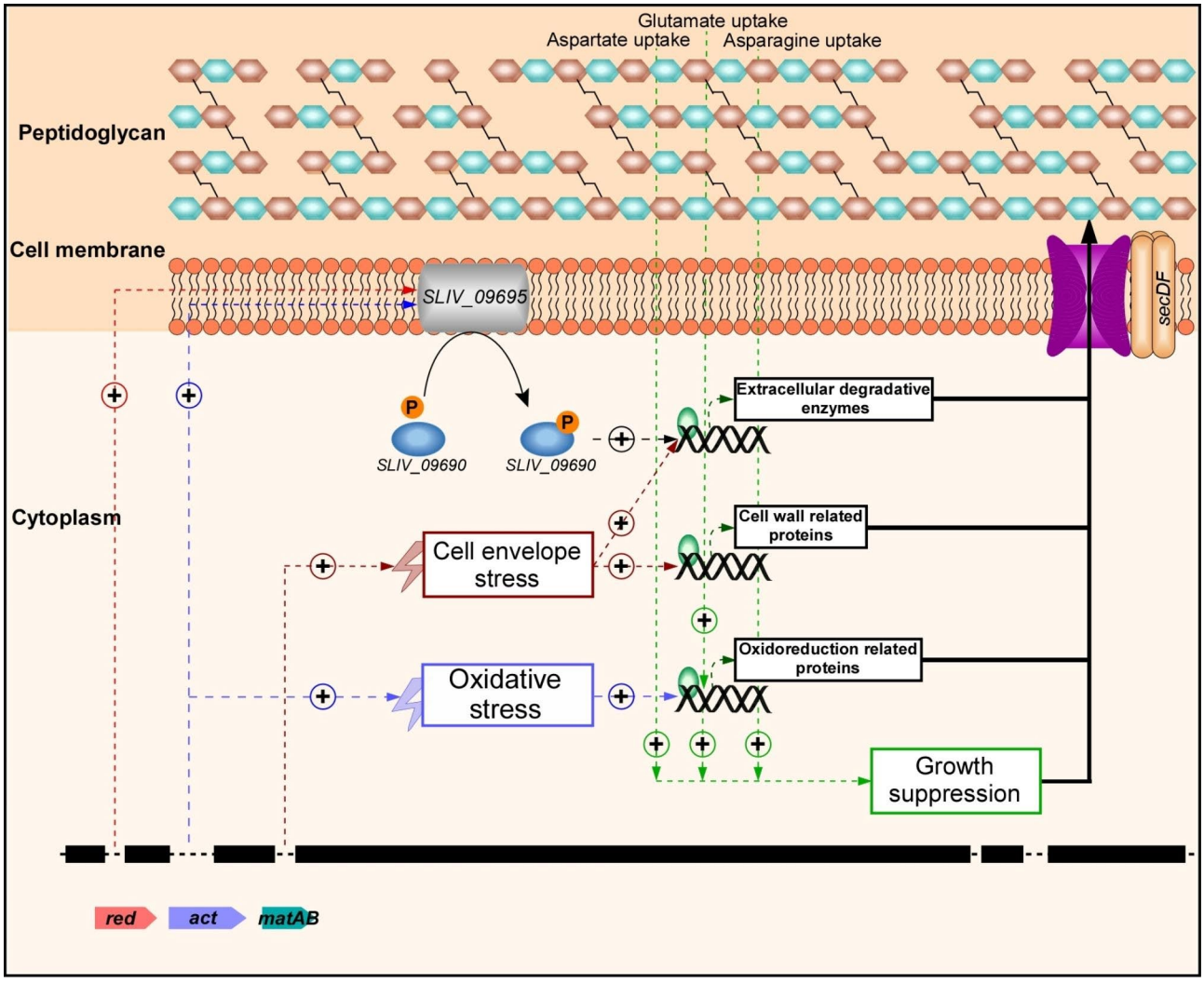


**Fig. 6** Proposed model for the effect of specialized metabolite clusters/ *matAB* deletion on protein secretion. Combined deletions of specialized metabolite clusters and *matAB* locus in *S. lividans* TK24 resulted in cells overexpressing and oversecreting proteins related to cell wall remodeling and oxidative stress. (+) indicates positive regulation

strains (1.5 and 1.9; both yielded the highest secretome mass; Fig. 3A).

Analysis of the spent growth medium of the parental and the RG strains by SDS-PAGE, showed a prominent band of ~27 kDa, close to the theoretical mRFP mass (25.4 kDa) (Fig. 5A; arrow) that was recognized by a rabbit polyclonal antibody raised against purified mRFP (Fig. 5B). To quantify mRFP secretion, His-mRFP, purified by metal affinity chromatography, was used to generate standard curves. These correlated either fluorescence measurements to protein mass (used in the left part of Fig. 5C) or signal intensity from immunodetection to protein mass (used in the right part of Fig. 5C) (see materials and methods; [3]). Using either quantification methods, we found that more mRFP was secreted by the RG strains than by the parental strain. After 24 h growth in NB medium, RG1.5 (51 mg/g DCW) and RG1.9 (79 mg/g DCW) secreted 25 and 70% respectively more mRFP than the parental strain (46 mg/g DCW) (Fig. 5C, right panel, compare lanes 3 and 5 to lane 1). After 48 h of growth, mRFP was only 8.5 and 24.5% more secreted by RG1.5 and RG1.9, respectively, than by the parental strain (Fig. 5C; right panel, compare lanes 6 and 4 to lane 2).

Using the same strategy we tested the secretion of mTNFα in the same strains. *S. lividans* TK24 and RG (1.5 and 1.9) strains expressing $sp^{SecV}$-*mTNFα*, were grown in NB medium for 24 h. Secreted proteins were TCA precipitated, analyzed by SDS-PAGE and silver-stained (Fig. S6A) or α-mTNF immunostained (Fig. S6B). To quantify the secreted protein, we generated standard curves that correlated the protein mass of purified his-mTNFα to signal intensity from immunodetection by specific antibodies [5]. The results showed that mTNFα was 11 and 31% more efficiently secreted by RG1.5 (195 mg/g DCW) and

RG1.9 (230 mg/g DCW), respectively, than by the parental strain (175 mg/g DCW) (Fig. S6C).

## Discussion

Our aim was to determine whether genome reduction in *S. lividans* TK24, that involved deletions, in combinations, of non-essential specialized metabolite gene clusters, of the gene encoding the sigma factor *hrdD* [68, 76, 77] and of the locus *matAB* encoding the putative polysaccharide synthases [77, 78] enhanced the overall secretome as well as the secretion of heterologous proteins.

Among the ten genome reduced strains we examined (Table 1) seven exhibited a minor reduction of biomass yield (Fig. 2A). The latter could be attributed to the rapid consumption and eventual depletion, by mid-exponential phase, of aspartate, glutamate and asparagine (Fig. S5; Table S7). For six of these strains, reduced biomass correlated with an overall enhanced ability to secrete proteins. Qualitative and quantitative changes were seen in the secretome of the RG strains compared to the parental one (Figs. 2 and 3 and S3; Table S3 and S4). The RG strains secreted 2–3 folds more polypeptides (Fig. 2A). In two of these RG strains (1.5 and 1.9) we recorded an increase in the secretion of two heterologous proteins (mRFP and mTNFα) compared to the parental strain (Fig. 5 and S5). Our data indicated that the stimulation of the secretion of native proteins also benefited to the secretion of heterologous proteins.

To gain insight into the metabolic changes caused by the combination of the various gene deletions, we performed comparative transcriptomics analysis of the parental and of one of the RG strains (RG1.9). This comparison revealed that 24 genes encoding proteins related to cell wall remodeling (biosynthesis/degradation) were upregulated in RG1.9 (Fig. 4B; Table S6). Among the 24 upregulated genes, four belonged to the $Sig^E$ regulon, that is known to control positively the expression of genes involved in cell wall synthesis [68] and negatively that of specialized metabolite biosynthetic clusters, like that of actinorhodin (Table S6). $sig^E$ deletions resulted in cell wall stress and actinorhodin overproduction in *S. coelicolor* [24, 79]. Consistently, this strain oversecreted > 13 proteins involved in cell wall remodeling as well as 3 proteins involved in stress response (Fig. 3B and D; Table S4). Twenty-nine genes encoding proteins with oxidation-reduction related function were upregulated in RG1.9. Eleven of them belonged to the $Sig^R$ regulon [69] such as organic hydroperoxide resistance protein *SLIV_22770* (*SCO2986*), putative thioesterase/thiol ester dehydratase-isomerase *SLIV_11095* (*SCO5482*) and thioredoxin reductase A *SLIV_18815* (SCO3890)] (Fig. 4B; Table S6). Altogether, our data suggested that both cell wall and oxidative stresses occur in RG1.9.

Even if further analysis is required to disentangle the contribution of each cluster/ gene to the observed phenotypes, we can propose that oxidative stress might be a consequence of the deletion of either the *act* cluster or/ and the *mel* gene since both actinorhodin and melanin were shown to act as antioxidants [63, 80–82]. Oxidative stress resulting from their absence might lead to cell wall damage. Alternatively, cell wall stress might have been caused by the deletion of *hrdD* or of the *matAB* locus. Indeed, in *S. coelicolor*, the transcription of *hrdD* is under the control of both $sig^E$ and $sig^R$, that are involved in sensing and responding to cell-wall [24] and thiol-oxidative [24] stresses, respectively, whereas the deletion of *matAB* is correlated with a thinner cell wall, lacking lamellae and patches and resulted into cell wall stress [78].

It has been proposed that Act can capture electrons of ROS/ NOS and of the respiratory chain [80]. These abilities are conferring to ACT anti-oxidant [80] and anti-respiratory functions [83]. The latter will have a negative impact on ATP generation. The deletion of ACT is thus predicted to lead to oxidative stress and enhanced ATP generation. The calcium ionophore antibiotic CDA, makes pores in the membrane and thus might dissipate the $H^+$ gradient resulting in the reduction of ATP generation by the ATP synthase [62, 80]. Similarly, an ATP spilling function was attributed to undecyprodigiosin (Red) in other bacteria [80]. We propose that the deletion of the *cda*, *red* and *act* clusters would lead to oxidative stress and enhanced ATP generation that might benefit the secretion process (Fig. 6).

Furthermore, enhanced oxidative stress, resulting from the deletions of the ACT cluster, the *mel* gene and the *matAB* locus, is predicted to lead to cell wall damages that would trigger the expression of the two-component system (*SLIV_09695* and *SLIV_09690*) (Fig. 6). The latter controls positively the expression of secreted enzymes involved in the degradation of damaged cell wall components [84–86]. The necessary re-modeling of the damaged cell wall would necessitate the specific up-take and consumption of the amino acids used for peptidoglycan biosynthesis (aspartate, glutamate and asparagine). The depletion in these amino acids could explain growth rate reduction and early entry into stationary phase that was observed in RG strains (Fig. 6).

In summary, by using a combination of proteomics, metabolomics, transcriptomics and protein secretion analyses, we provided an in-depth view of the complex metabolic changes that resulted from deletions of specialized metabolite clusters and of *matAB* and *hrdD* genes. These changes are accompanied by the over expression of secretory chaperones and of components of the secretory system such as the SecDF that are likely to contribute positively to the significantly enhanced secretion of native as well as heterologous proteins. Our study

revealed the existence of complex regulatory networks linking specialized metabolite production and protein secretion.

## Supplementary Information

The online version contains supplementary material available at https://doi.org/10.1186/s12934-023-02269-x.

Supplementary Material 1

Supplementary Material 2

Supplementary Material 3

Supplementary Material 4

Supplementary Material 5

Supplementary Material 6

Supplementary Material 7

**Acknowledgements**
We thank Clara Marcelín-Leyva for preliminary experiments. This study was supported by: the European Union project (grant QLK3-CT-2002-02056, QLK3-LSHG-CT-2007-037586 and E.U.-FP7 project 613877 to JK, JA and AE); by the FWO (Fund for Scientific Research – Flanders); grant research project RiMembR (#G0C6814N) and by FWO/F.R.S.-FNRS ProFlow ("Excellence of Science - EOS" programme grant #30550343) to AE); RUN (#RUN/16/001 KU Leuven to AE); PROFOUND (W002421N; WoG/FWO) FOscil (ZKD4582 - C16/18/008; KU Leuven) to AE and SK): and by the Slovak Academy of Sciences (VEGA grant 2/00026/20 to JK). The Egyptian government doctoral scholar.

**Author contribution**
HMB Designed and performed experiments of cell growth, protoplast preparation/ transformation, protein secretion, transcriptomics and proteomics experiments/data analysis and figures preparation; BT and KJ performed transcriptomics analysis; SK and BK designed/ performed/ analyzed metabolomics experiments; JK constructed reduced genome strains; VML supplied plasmids; AJ and CS analyzed data; EA and KS conceived and managed the project; HMD wrote the first draft of the paper; HMB, KS and EA wrote, corrected and finalized the paper. All authors read and approved the MS.

**Funding**
This study was supported by: the European Union project (grant QLK3-CT-2002-02056, QLK3-LSHG-CT-2007-037586 and E.U.-FP7 project 613877 to JK, JA and AE); by the FWO (Fund for Scientific Research – Flanders) grant research project RiMembR (#G0C6814N) and the FWO/F.R.S.-FNRS ProFlow ("Excellence of Science - EOS" programme grant #30550343 to AE); RUN (#RUN/16/001 KU Leuven to AE); PROFOUND (W002421N; WoG/FWO) FOscil (ZKD4582 - C16/18/008; KU Leuven to AE and SK): and by the Slovak Academy of Sciences (VEGA grant 2/00026/20 to JK). The Egyptian government supported HMB with a doctoral scholarship.

**Data Availability**
All relevant data will be deposited in public repositories and all materials will be made available upon request.

## Declarations

**Ethics approval and consent to participate**
Not applicable.

**Consent for publication**
• All authors of the manuscript have read and agreed to its content and are accountable for all aspects of the accuracy and integrity of the manuscript in accordance with ICMJE criteria.
• The manuscript is original, has not already been published, and is not currently under consideration by another journal.
• You agree to the terms of the BioMed Central License Agreement and Open data policy, which you have read. For authors who are prevented from being copyright holders (for instance where Crown Copyright applies or researchers are US government employees) BioMed Central can accommodate nonstandard copyright lines. If this applies to you, please contact us and provide details of your situation.
• By submitting your article for consideration, you acknowledge that, where your institution or funder has a BioMed Central membership, we may refer your name and contact details to a representative of that organisation in order for us to verify whether it agrees to cover, in full or in part, the article processing charge (APC) that is payable upon editorial acceptance of submitted articles.
Yes, I am the author responsible for the submission and the BioMed Central License Agreement as detailed above.

**Competing interests**
The authors declare no competing interests.

Received: 26 July 2023 / Accepted: 10 December 2023
Published online: 05 January 2024

**References**

1. Tarkka M, Hampp R. Secondary Metabolites of Soil *Streptomycetes* in Biotic Interactions. In *Secondary Metabolites in Soil Ecology* Edited by Karlovsky P. Berlin, Heidelberg: Springer Berlin Heidelberg; 2008: 107–126.[*Soil Biology*].
2. Hamed MB, Karamanou S, Olafsdottir S, Basilio JSM, Simoens K, Tsolis KC, Van Mellaert L, Guethmundsdottir EE, Hreggvidsson GO, Anne J, et al. Large-scale production of a thermostable *Rhodothermus marinus* cellulase by heterologous secretion from *Streptomyces lividans*. Microb Cell Fact. 2017;16:232.
3. Hamed MB, Vrancken K, Bilyk B, Koepff J, Novakova R, van Mellaert L, Oldiges M, Luzhetskyy A, Kormanec J, Anne J, et al. Monitoring protein secretion in *Streptomyces* using fluorescent proteins. Front Microbiol. 2018;9:3019.
4. Lammertyn E, Van Mellaert L, Schacht S, Dillen C, Sablon E, Van Broekhoven A, Anne J. Evaluation of a novel subtilisin inhibitor gene and mutant derivatives for the expression and secretion of mouse Tumor necrosis factor alpha by *Streptomyces lividans*. Appl Environ Microbiol. 1997;63:1808–13.
5. Pozidis C, Lammertyn E, Politou AS, Anne J, Tsiftsoglou AS, Sianidis G, Economou A. Protein secretion biotechnology using *Streptomyces lividans*: large-scale production of functional trimeric Tumor necrosis factor alpha. Biotechnol Bioeng. 2001;72:611–9.
6. Sianidis G, Pozidis C, Becker F, Vrancken K, Sjoeholm C, Karamanou S, Takamiya-Wik M, van Mellaert L, Schaefer T, Anne J, Economou A. Functional large-scale production of a novel Jonesia sp. xyloglucanase by heterologous secretion from *Streptomyces lividans*. J Biotechnol. 2006;121:498–507.
7. Tao X, Zhao M, Zhang Y, Liu M, Liu Q, Wang W, Wang FQ, Wei D. Comparison of the expression of phospholipase D from Streptomyces halstedii in different hosts and its over-expression in *Streptomyces lividans*. FEMS Microbiol Lett 2019, 366.
8. Cavaletti L, Taravella A, Carrano L, Carenzi G, Sigurta A, Solinas N, Caro S, Stasio LD, Picascia S, Laezza M, et al. E40, a novel microbial protease efficiently detoxifying gluten proteins, for the dietary management of gluten intolerance. Sci Rep. 2019;9:13147.
9. Cihak M, Kamenik Z, Smidova K, Bergman N, Benada O, Kofronova O, Petrickova K, Bobek J. Secondary metabolites produced during the germination of *Streptomyces coelicolor*. Front Microbiol. 2017;8:2495.
10. Zhang Z, Pan HX, Tang GL. New insights into bacterial type II polyketide biosynthesis. F1000Res. 2017;6:172.
11. Payne JA, Schoppet M, Hansen MH, Cryle MJ. Diversity of nature's assembly lines - recent discoveries in non-ribosomal peptide synthesis. Mol Biosyst. 2016;13:9–22.
12. Gokulan K, Khare S, Cerniglia C. METABOLIC PATHWAYS | production of secondary metabolites of Bacteria. In Encyclopedia of Food Microbiology 2014: 561–9.
13. Tzin V, Galili G. The Biosynthetic pathways for Shikimate and aromatic amino acids in *Arabidopsis thaliana*. Arabidopsis Book. 2010;8:e0132.
14. García-Estrada C, Domínguez-Santos R, Kosalková K, Martín J-F. Transcription factors Controlling Primary and secondary metabolism in filamentous Fungi: the β-Lactam paradigm. Fermentation. 2018;4:47.

15. Sola-Landa A, Moura RS, Martin JF. The two-component PhoR-PhoP system controls both primary metabolism and secondary metabolite biosynthesis in *Streptomyces lividans*. Proc Natl Acad Sci U S A. 2003;100:6133–8.
16. Liu G, Chater KF, Chandra G, Niu G, Tan H. Molecular regulation of antibiotic biosynthesis in *streptomyces*. Microbiol Mol Biol Rev. 2013;77:112–43.
17. Ruckert C, Albersmeier A, Busche T, Jaenicke S, Winkler A, Friethjonsson OH, Hreggviethsson GO, Lambert C, Badcock D, Bernaerts K, et al. Complete genome sequence of *Streptomyces lividans* TK24. J Biotechnol. 2015;199:21–2.
18. Droste J, Busche T, Rückert C, Hamed MB, Anné J, Simoens K, Bernaerts K, Economou A, Kalinowski J. Extensive reannotation of the genome of the model Streptomycete *Streptomyces lividans* TK24 based on transcriptome and proteome information. *submitted* 2020.
19. Hamed MB, Anne J, Karamanou S, Economou A. *Streptomyces* protein secretion and its application in biotechnology. FEMS Microbiol Lett 2018, 365.
20. Bentley SD, Chater KF, Cerdeno-Tarraga AM, Challis GL, Thomson NR, James KD, Harris DE, Quail MA, Kieser H, Harper D, et al. Complete genome sequence of the model actinomycete *Streptomyces coelicolor* A3(2). Nature. 2002;417:141–7.
21. Sevcikova B, Kormanec J. Differential production of two antibiotics of *Streptomyces coelicolor* A3(2), actinorhodin and undecylprodigiosin, upon salt stress conditions. Arch Microbiol. 2004;181:384–9.
22. Wei J, He L, Niu G. Regulation of antibiotic biosynthesis in actinomycetes: perspectives and challenges. Synth Syst Biotechnol. 2018;3:229–35.
23. Fujii T, Gramajo HC, Takano E, Bibb MJ. redD and actII-ORF4, pathway-specific regulatory genes for antibiotic production in *Streptomyces coelicolor* A3(2), are transcribed in vitro by an RNA polymerase holoenzyme containing sigma hrdD. J Bacteriol. 1996;178:3402–5.
24. Rebets Y, Tsolis KC, Guethmundsdottir EE, Koepff J, Wawiernia B, Busche T, Bleidt A, Horbal L, Myronovskyi M, Ahmed Y, et al. Characterization of Sigma factor genes in *Streptomyces lividans* TK24 using a genomic Library-Based Approach for multiple gene deletions. Front Microbiol. 2018;9:3033.
25. Sun D, Liu C, Zhu J, Liu W. Connecting metabolic pathways: Sigma factors in *Streptomyces* spp. Front Microbiol. 2017;8:2546.
26. Huang J, Lih CJ, Pan KH, Cohen SN. Global analysis of growth phase responsive gene expression and regulation of antibiotic biosynthetic pathways in *Streptomyces coelicolor* using DNA microarrays. Genes Dev. 2001;15:3183–92.
27. Jeong Y, Kim JN, Kim MW, Bucca G, Cho S, Yoon YJ, Kim BG, Roe JH, Kim SC, Smith CP, Cho BK. The dynamic transcriptional and translational landscape of the model antibiotic producer *Streptomyces coelicolor* A3(2). Nat Commun. 2016;7:11605.
28. Posfai G, Plunkett G 3rd, Feher T, Frisch D, Keil GM, Umenhoffer K, Kolisnychenko V, Stahl B, Sharma SS, de Arruda M, et al. Emergent properties of reduced-genome *Escherichia coli*. Science. 2006;312:1044–6.
29. Csorgo B, Feher T, Timar E, Blattner FR, Posfai G. Low-mutation-rate, reduced-genome *Escherichia coli*: an improved host for faithful maintenance of engineered genetic constructs. Microb Cell Fact. 2012;11:11.
30. Choe D, Lee JH, Yoo M, Hwang S, Sung BH, Cho S, Palsson B, Kim SC, Cho BK. Adaptive laboratory evolution of a genome-reduced *Escherichia coli*. Nat Commun. 2019;10:935.
31. Kurokawa M, Seno S, Matsuda H, Ying BW. Correlation between genome reduction and bacterial growth. DNA Res. 2016;23:517–25.
32. Morimoto T, Kadoya R, Endo K, Tohata M, Sawada K, Liu S, Ozawa T, Kodama T, Kakeshita H, Kageyama Y, et al. Enhanced recombinant protein productivity by genome reduction in *Bacillus subtilis*. DNA Res. 2008;15:73–81.
33. Manabe K, Kageyama Y, Morimoto T, Ozawa T, Sawada K, Endo K, Tohata M, Ara K, Ozaki K, Ogasawara N. Combined effect of improved cell yield and increased specific productivity enhances recombinant enzyme production in genome-reduced *Bacillus subtilis* strain MGB874. Appl Environ Microbiol. 2011;77:8370–81.
34. Zhu D, Fu Y, Liu F, Xu H, Saris PE, Qiao M. Enhanced heterologous protein productivity by genome reduction in *Lactococcus lactis* NZ9000. Microb Cell Fact. 2017;16:1.
35. Rezuchova B, Homerova D, Sevcikova B, Nunez LE, Novakova R, Feckova L, Skultety L, Cortes J, Kormanec J. An efficient blue-white screening system for markerless deletions and stable integrations in *Streptomyces* chromosomes based on the blue pigment indigoidine biosynthetic gene bpsA. Appl Microbiol Biotechnol. 2018;102:10231–44.
36. Ahmed Y, Rebets Y, Estevez MR, Zapp J, Myronovskyi M, Luzhetskyy A. Engineering of *Streptomyces lividans* for heterologous expression of secondary metabolite gene clusters. Microb Cell Fact. 2020;19:5.
37. Busche T, Tsolis KC, Koepff J, Rebets Y, Ruckert C, Hamed MB, Bleidt A, Wiechert W, Lopatniuk M, Yousra A, et al. Multi-omics and targeted approaches to determine the role of Cellular proteases in *Streptomyces* Protein Secretion. Front Microbiol. 2018;9:1174.
38. Novakova R, Nunez LE, Homerova D, Knirschova R, Feckova L, Rezuchova B, Sevcikova B, Menendez N, Moris F, Cortes J, Kormanec J. Increased heterologous production of the antitumoral polyketide mithramycin A by engineered *Streptomyces lividans* TK24 strains. Appl Microbiol Biotechnol. 2018;102:857–69.
39. Zhou M, Jing X, Xie P, Chen W, Wang T, Xia H, Qin Z. Sequential deletion of all the polyketide synthase and nonribosomal peptide synthetase biosynthetic gene clusters and a 900-kb subtelomeric sequence of the linear chromosome of *Streptomyces coelicolor*. FEMS Microbiol Lett. 2012;333:169–79.
40. Gomez-Escribano JP, Bibb MJ. Engineering *Streptomyces coelicolor* for heterologous expression of secondary metabolite gene clusters. Microb Biotechnol. 2011;4:207–15.
41. Mani I, Sharma V, Tamboli I, Raman G. Interaction of melanin with proteins–the importance of an acidic intramelanosomal pH. Pigment Cell Res. 2001;14:170–9.
42. Koepff J, Keller M, Tsolis KC, Busche T, Ruckert C, Hamed MB, Anne J, Kalinowski J, Wiechert W, Economou A, Oldiges M. Fast and reliable strain characterization of *Streptomyces lividans* through micro-scale cultivation. Biotechnol Bioeng. 2017;114:2011–22.
43. Kieser T, Bibb MJ, Buttner MJ, Chater KF, Hopwood DA. Practical Streptomyces genetics. Norwich, UK.: John Innes Foundation; 2000.
44. Anne J, Van Mellaert L, Eyssen H. Optimum conditions for efficient transformation of *Streptomyces venezuelae* protoplasts. Appl Microbiol Biotechnol. 1990;32:431–5.
45. Tsolis KC, Hamed MB, Simoens K, Koepff J, Busche T, Ruckert C, Oldiges M, Kalinowski J, Anne J, Kormanec J, et al. Secretome Dynamics in a gram-positive bacterial model. Mol Cell Proteomics. 2019;18:423–36.
46. Hamed MB, El-Badry MO, Kandil EI, Borai IH, Fahmy AS. A contradictory action of procoagulant ficin by a fibrinolytic serine protease from Egyptian *Ficus carica* latex. Biotechnol Rep (Amst). 2020;27:e00492.
47. Abdel-Aty AM, Hamed MB, Gad AAM, El-Hakim AE, Mohamed SA. *Ficus sycomorus* latex: an efficient alternative Egyptian source for horseradish peroxidase in labeling with antibodies for immunodiagnostic kits. Vet World. 2018;11:1364–70.
48. Rappsilber J, Mann M, Ishihama Y. Protocol for micro-purification, enrichment, pre-fractionation and storage of peptides for proteomics using StageTips. Nat Protoc. 2007;2:1896–906.
49. Tsolis KC, Economou A. Quantitative proteomics of the *E. Coli* Membranome. Methods Enzymol. 2017;586:15–36.
50. Schwanhausser B, Busse D, Li N, Dittmar G, Schuchhardt J, Wolf J, Chen W, Selbach M. Global quantification of mammalian gene expression control. Nature. 2011;473:337–42.
51. Benjamini Y, Hochberg Y. Controlling the false Discovery Rate - a practical and powerful Approach to multiple testing. J Royal Stat Soc Ser B-Statistical Methodol. 1995;57:289–300.
52. Tsolis KC, Tsare EP, Orfanoudaki G, Busche T, Kanaki K, Ramakrishnan R, Rousseau F, Schymkowitz J, Ruckert C, Kalinowski J, et al. Comprehensive subcellular topologies of polypeptides in *Streptomyces*. Microb Cell Fact. 2018;17:43.
53. Jiang L, Liu Y, Wang P, Wen Y, Song Y, Chen Z, Li J. Inactivation of the extracytoplasmic function sigma factor Sig6 stimulates avermectin production in *Streptomyces avermitilis*. Biotechnol Lett. 2011;33:1955–61.
54. Busche T, Winkler A, Wedderhoff I, Ruckert C, Kalinowski J, Ortiz de Orue Lucana D. Deciphering the transcriptional response mediated by the Redox-Sensing System HbpS-SenS-SenR from Streptomycetes. PLoS ONE. 2016;11:e0159873.
55. Busche T, Silar R, Picmanova M, Patek M, Kalinowski J. Transcriptional regulation of the operon encoding stress-responsive ECF sigma factor SigH and its anti-sigma factor RshA, and control of its regulatory network in *Corynebacterium glutamicum*. BMC Genomics. 2012;13:445.
56. Daniels W, Bouvin J, Busche T, Ruckert C, Simoens K, Karamanou S, Van Mellaert L, Friethjonsson OH, Nicolai B, Economou A, et al. Transcriptomic and fluxomic changes in *Streptomyces lividans* producing heterologous protein. Microb Cell Fact. 2018;17:198.
57. Love MI, Huber W, Anders S. Moderated estimation of Fold change and dispersion for RNA-seq data with DESeq2. Genome Biol. 2014;15:550.
58. Mortazavi A, Williams BA, McCue K, Schaeffer L, Wold B. Mapping and quantifying mammalian transcriptomes by RNA-Seq. Nat Methods. 2008;5:621–8.
59. Hilker R, Stadermann KB, Schwengers O, Anisiforov E, Jaenicke S, Weisshaar B, Zimmermann T, Goesmann A. ReadXplorer 2-detailed read mapping analysis and visualization from one single source. Bioinformatics. 2016;32:3702–8.

60. Vizcaino JA, Csordas A, Del-Toro N, Dianes JA, Griss J, Lavidas I, Mayer G, Perez-Riverol Y, Reisinger F, Ternent T, et al. 2016 update of the PRIDE database and its related tools. Nucleic Acids Res. 2016;44:11033.
61. Krause J, Handayani I, Blin K, Kulik A, Mast Y. Disclosing the potential of the SARP-Type Regulator PapR2 for the activation of antibiotic gene clusters in Streptomycetes. Front Microbiol. 2020;11:225.
62. Ryding NJ, Anderson TB, Champness WC. Regulation of the *Streptomyces coelicolor* calcium-dependent antibiotic by absA, encoding a cluster-linked two-component system. J Bacteriol. 2002;184:794–805.
63. Lejeune C, Sago L, Cornu D, Redeker V, Virolle MJ. A proteomic analysis indicates that oxidative stress is the common feature triggering antibiotic production in Streptomyces coelicolor and in the pptA mutant of *Streptomyces lividans*. Front Microbiol. 2021;12:813993.
64. Benjamini Y, Hochberg Y. Controlling the false discovery rate: a practical and powerful approach to multiple hypothesis testing. J R Stat Soc B 1995, 57.
65. Sobczyk A, Bellier A, Viala J, Mazodier P. The lon gene, encoding an ATP-dependent protease, is a novel member of the HAIR/HspR stress-response regulon in actinomycetes. Microbiol (Reading). 2002;148:1931–7.
66. Stefankova P, Maderova J, Barak I, Kollarova M, Otwinowski Z. Expression, purification and X-ray crystallographic analysis of thioredoxin from *Streptomyces coelicolor*. Acta Crystallogr Sect F Struct Biol Cryst Commun. 2005;61:164–8.
67. Urem M, Rossum Tv, Bucca G, Moolenaar GF, Laing E, Świątek-Połatyńska MA, Willemse J, Tenconi E, Rigali S, Goosen N, et al. OsdR of *Streptomyces coelicolor* and the Dormancy Regulator DevR of *Mycobacterium tuberculosis* Control overlapping regulons. mSystems. 2016;1. https://doi.org/10.1128/mSystems.00014-16.
68. Tran NT, Huang X, Hong HJ, Bush MJ, Chandra G, Pinto D, Bibb MJ, Hutchings MI, Mascher T, Buttner MJ. Defining the regulon of genes controlled by sigma(E), a key regulator of the cell envelope stress response in *Streptomyces coelicolor*. Mol Microbiol. 2019;112:461–81.
69. Paget MS, Molle V, Cohen G, Aharonowitz Y, Buttner MJ. Defining the disulphide stress response in Streptomyces coelicolor A3(2): identification of the sigmaR regulon. Mol Microbiol. 2001;42:1007–20.
70. Botas A, Perez-Redondo R, Rodriguez-Garcia A, Alvarez-Alvarez R, Yague P, Manteca A, Liras P. ArgR of *Streptomyces coelicolor* is a pleiotropic Transcriptional Regulator: Effect on the Transcriptome, Antibiotic Production, and differentiation in liquid cultures. Front Microbiol. 2018;9:361.
71. De Keersmaeker S, Van Mellaert L, Schaerlaekens K, Van Dessel W, Vrancken K, Lammertyn E, Anne J, Geukens N. Structural organization of the twin-arginine translocation system in *Streptomyces lividans*. FEBS Lett. 2005;579:797–802.
72. Schaerlaekens K, Schierova M, Lammertyn E, Geukens N, Anne J, Van Mellaert L. Twin-arginine translocation pathway in *Streptomyces lividans*. J Bacteriol. 2001;183:6727–32.
73. Widdick DA, Dilks K, Chandra G, Bottrill A, Naldrett M, Pohlschroder M, Palmer T. The twin-arginine translocation pathway is a major route of protein export in *Streptomyces coelicolor*. Proc Natl Acad Sci U S A. 2006;103:17927–32.
74. Guimond J, Morosoli R. Identification of *Streptomyces lividans* proteins secreted by the twin-arginine translocation pathway following growth with different carbon sources. Can J Microbiol. 2008;54:549–58.
75. Valverde JR, Gullon S, Garcia-Herrero CA, Campoy I, Mellado RP. Dynamic metabolic modelling of overproduced protein secretion in *Streptomyces lividans* using adaptive DFBA. BMC Microbiol. 2019;19:233.
76. Yamazaki H, Ohnishi Y, Horinouchi S. Transcriptional switch on of *ssgA* by A-factor, which is essential for spore septum formation in *Streptomyces griseus*. J Bacteriol. 2003;185:1273–83.
77. van Dissel D, Claessen D, Roth M, van Wezel GP. A novel locus for mycelial aggregation forms a gateway to improved *Streptomyces* cell factories. Microb Cell Fact. 2015;14:44.
78. Ultee E, van der Aart LT, Zhang L, van Dissel D, Diebolder CA, van Wezel GP, Claessen D, Briegel A. Teichoic acids anchor distinct cell wall lamellae in an apically growing bacterium. Commun Biol. 2020;3:314.
79. Paget MS, Chamberlin L, Atrih A, Foster SJ, Buttner MJ. Evidence that the extracytoplasmic function sigma factor sigmaE is required for normal cell wall structure in *Streptomyces coelicolor* A3(2). J Bacteriol. 1999;181:204–11.
80. Virolle MJ. A challenging view: antibiotics play a role in the regulation of the energetic metabolism of the producing Bacteria. Antibiot (Basel) 2020, 9.
81. Millan-Oropeza A, Henry C, Lejeune C, David M, Virolle MJ. Expression of genes of the pho regulon is altered in *Streptomyces coelicolor*. Sci Rep. 2020;10:8492.
82. de Cassia RGR, Pombeiro-Sponchiado SR. Antioxidant activity of the melanin pigment extracted from *aspergillus nidulans*. Biol Pharm Bull. 2005;28:1129–31.
83. Esnault C, Dulermo T, Smirnov A, Askora A, David M, Deniset-Besseau A, Holland IB, Virolle MJ. Strong antibiotic production is correlated with highly active oxidative metabolism in *Streptomyces coelicolor* M145. Sci Rep. 2017;7:200.
84. Rozas D, Gullón S, Mellado RP. A novel two-component system involved in the transition to secondary metabolism in *Streptomyces coelicolor*. PLoS ONE. 2012;7:e31760.
85. Rodríguez H, Rico S, Díaz M, Santamaría RI. Two-component systems in Streptomyces: key regulators of antibiotic complex pathways. Microb Cell Fact. 2013;12:127.
86. Mäder U, Antelmann H, Buder T, Dahl MK, Hecker M, Homuth G. *Bacillus subtilis* functional genomics: genome-wide analysis of the DegS-DegU regulon by transcriptomics and proteomics. Mol Genet Genomics. 2002;268:455–67.


## Publisher's Note